

A fiber placement device and methodology for preparing 2-D and 3-D combinatorial microcomposites

J. H. Kim · J. W. Hettenhouser · C. K. Moon ·
G. A. Holmes

Received: 14 October 2008 / Accepted: 18 February 2009 / Published online: 5 May 2009
© Springer Science+Business Media, LLC 2009

Abstract A fiber placement device is described and methodology is given for preparing two-dimensional (2-D) and three-dimensional (3-D) combinatorial microcomposites. Although 2-D microcomposites with uniform fiber spacing have been prepared previously, the preparation of uniformly spaced 3-D microcomposites with 6–20 μm diameter fibers is new. The preparation of these combinatorial specimens was motivated by research results from reference [Li et al. (1995) Compos Sci Technol 54:251]. These results showed that the mean fragment length of the broken fibers in an array of fibers of the shear-lag models increases as the inter-fiber separation decreases. It was noted that shear-lag theory predicts the opposite effect. Therefore, specimens of this type are needed to unambiguously verify this trend. In addition, data from this new technology should delineate the factors that influence critical flaw nucleation in unidirectional laminate composites.

Introduction

The theoretical prediction of composite failure is generally based on *chain-of-bundles* (δ -bundle) models that account for the strength variability of the reinforcing fibers. The single fiber fragmentation test (SFFT) and the single fiber test (SFT) have been the preferred test methodologies for obtaining input parameters for these models. Recent research [1], however, indicates that the estimate of the Weibull shape parameter obtained from the SFFT better approximates the strength of a unidirectional (UD) composite lamina than the Weibull parameter obtained from the SFT. However, when the validity of the SFFT Weibull parameter was checked by predicting the distribution of fragment lengths that arises from the SFFT, only a fair agreement was obtained [2].

In the composite failure models developed by Rosen et al. [3–5] in 1964, two-dimensional (2-D) microcomposites were used to obtain the input data. However, these and other early research efforts [6–8] were characterized primarily by the use of large diameter fibers that fractured at random locations as the load in the microcomposite was increased. Although tedious to prepare, recent 2-D microcomposite research [9–20] using fibers, whose diameter is 5–20 μm are comparable to those found in typical composite lamina, and have shown that the interaction of closely spaced fibers results in the clustering of fiber breaks (nonrandom fracture) due to the interaction between broken and nonbroken fibers. An often overlooked result from these research efforts [9] is the observation that the fiber fragment length distribution from saturated 2-D microcomposites have a larger mean fragment length than saturated single fibers from the SFFT. This research also shows that the fragment length increases with smaller inter-fiber separation or more embedded fibers. Shear-lag theory,

This paper is declared as a work of the U.S. Government and is not subject to copyright protection in the United States.

J. H. Kim · C. K. Moon · G. A. Holmes (✉)
National Institute of Standards and Technology, Polymers
Division, Characterization and Methods Development Group,
100 Bureau Drive Stop 8541, Gaithersburg, MD 20899-8541,
USA
e-mail: gale.holmes@nist.gov

J. W. Hettenhouser
Fabrication Technology Division, Shops 100 Bureau Drive Stop
8250, Gaithersburg, MD 20899-8250, USA

Present Address:
C. K. Moon
Materials Science and Engineering, College of Engineering,
Pukyong National University, San 100, Yongdang-Dong,
Nam-Gu, Busan 608-738, Korea

which forms the basis for most composite failure models, predicts the opposite effect [9].

Noting that the SFFT is also used to obtain the flaw distribution and the in situ fiber strength in the matrix, these above results have led some researchers to suggest that this test procedure is not an effective methodology for obtaining input parameters for the Cox–Hedgepeth-type shear-lag-based composite failure models. This is especially true since these shear-lag models do not appear to account accurately for the effect of fiber–fiber interactions. As a result, modeling studies [21–24] and the testing of 2-D microcomposite have emerged as alternative approaches for obtaining these parameters. An interesting theoretical result by Smith et al. [25] suggests that the experimental data from 2-D micro-composites that connect the Weibull shape parameter to the critical failure sequence size in composite failure models do not in general hold for 3-D microcomposites. However, the preparation of 3-D microcomposites to verify this result has been hampered by complicated and nonreproducible preparation procedures [26]. These results underscore the need to completely understand the micromechanics of composite failure behavior and suggest that a reproducible methodology for preparing 3-D microcomposites may be an essential tool for achieving this goal.

Because all multifiber arrays are tedious to prepare, we discuss in this article a device that facilitates the preparation of uniform and closely spaced 2-D fiber arrays (approximately 1 fiber diameter) and the extension of this approach to the preparation of uniform 3-D fiber arrays. In addition, methodologies are advanced for placing these arrays precisely in a silicone mold and the preparation of combinatorial-type specimens that allows for the simultaneous testing of single-fiber composites and multifiber arrays.

Design

The design presented in this article, borrows largely from Wagner and Steenbakkers’s device [10] that uses the synchronized rotation of the fiber guides to control the inter-fiber spacings in the fiber arrays. The device described in this report incorporates this approach but includes several key changes to facilitate the preparation of uniform and closely spaced 2-D and 3-D multifiber arrays. First, the two fiber guides (i.e., fiber pin blocks) are attached to the central gear using backlash gears (see Figs. 1, 2). This controls the synchronous rotation of the fiber pin blocks and reduces the variability between these blocks during the rotation process. A thumb wheel gear via a connecting pinion gear rotates the central gear. After the fibers are rotated to the desired inter-fiber distance, the thumb wheel is held at that location using a stop screw.

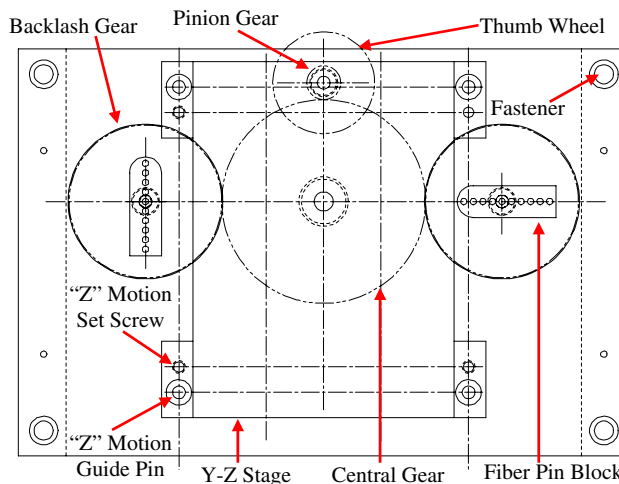


Fig. 1 Top view of fiber-setting device with gear assembly

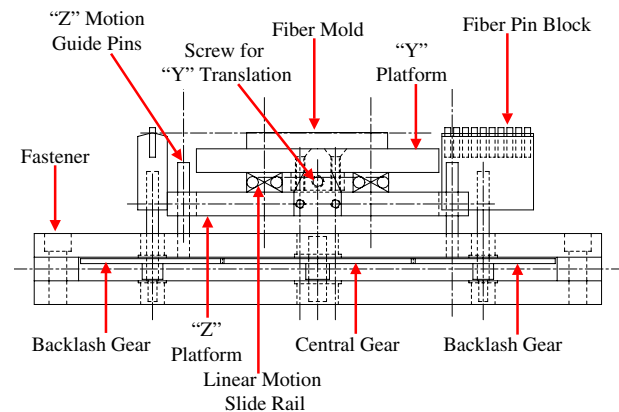


Fig. 2 Side view of fiber-setting device with gear assembly

In an earlier design of the fiber pin block, the holes were drilled into the diameter of the guide pins, and the pins were secured with glue. This approach resulted in a distortion in the uniform spacing between adjacent fibers at very small inter-fiber distances. To reduce this distortion in the inter-fiber spacing of the array, several modifications were made to the fiber pin block. The holes for the 5.715 mm (0.225 in) diameter fiber guides were drilled at a slightly smaller diameter 5.588 mm (0.220 in), to a depth of 12.7 mm (0.500 in), and with an inter-guide center-to-center distance of 4.7625 ± 0.0127 mm (0.1875 ± 0.0005 in). To accommodate the 5.715 mm (0.225 in) fiber guides, the fiber pin block was then heated approximately to 500 °C to expand the diameter of the holes, thereby achieving a press fit of the guide pins in the drilled holes (see Fig. 3). Second, the flat surface of the fiber pin block was replaced with a triangular surface that comes to a point at the center of the holes for the guide pins. This modification allows the fibers to rotate freely when the inter-fiber spacing is small (see Fig. 3).

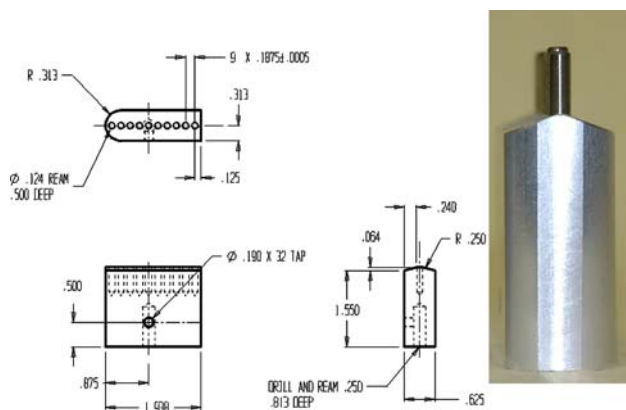


Fig. 3 Schematics of fiber pin block. Inset shows triangular surfacing away from fiber pins; this modification helps maintain array uniformity at small inter-fiber spacings

In another departure from Wagner and Steenbakkers' device, a stage with “Y” and “Z” motion was placed between the two fiber pin blocks to hold the silicone mold (see Figs. 1, 2). The “Y” motion of the stage was achieved by mounting the top (“Y”) platform of the stage on two Del-Tron 5” linear motion slide rails.¹ Mounting a screw drive to the “Y” platform controlled translation in the “Y” direction. This motion allows the position of the fiber array to be adjusted precisely within a cavity of the silicone mold. The “Z” motion was obtained by mounting the bottom (“Z”) platform of the stage on four guide pins. The “Z” motion height is controlled by four set screws.

To secure the single fibers in place prior to gluing them in the mold, two beams that parallel the “Y” direction (i.e., the lengthwise direction of the mold) are secured on the top platform of the stage (not shown in Figs. 1, 2, shown in Fig. 4). Consistent with previous laboratory practice, double-sided stick tape is then placed on the two steel beams.

The preparation of eight-cavity silicone molds has been described previously [27, 28]. The mold used here is similar but contains two channels on each side of the mold cavities that run parallel to the “Y” direction of the mold. These additions facilitate the preparation of 3-D microcomposites (see Fig. 4).

Methodology for preparing 2-D, combinatorial, and 3-D microcomposites

The fiber pin blocks are adjusted on the fiber placement device to be parallel and are then secured with set screws.

¹ Certain commercial materials and equipments are identified in this article in order to specify adequately the experimental procedure. In no case, does such identification imply recommendation or endorsement by the National Institute of Standards and Technology, nor does it imply necessarily that the items are the best available for the purpose.

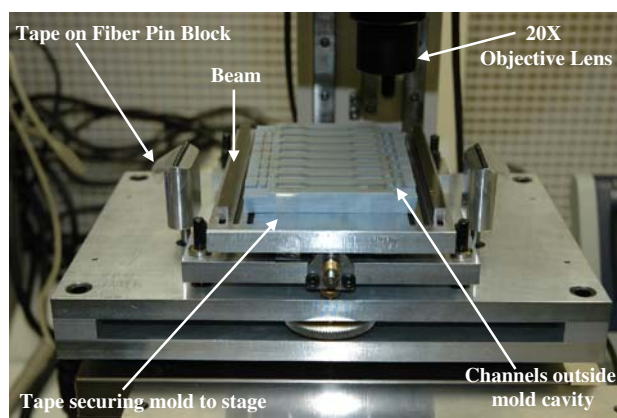


Fig. 4 Fiber-setting device on MM-40 measurescope stage

Although the fiber-setting device, as modified, can be used in conjunction with the weight stands employed by Wagner and Steenbakkers to pre-tension the fibers, tension is maintained on the fibers in this research by placing double-sided stick tape on the outside of each fiber pin block (see Fig. 4). With the stage in its lowest position, a mold is placed on the stage. Using a Laminare hood as the sample preparation area, the fibers are then stretched across each fiber pin and temporarily secured onto the tape. After all of the fibers are in place, another piece of tape is placed on top of the fibers to secure them in place, but not too tight to prevent slippage of the fibers between the tape as the fiber pin blocks are rotated. The slippage is necessary to prevent any breakage of the fibers during rotation.

To achieve the desired inter-fiber spacing, the stage is placed onto the X–Y stage of a Nikon MM-40 measuring microscope (measurescope), also in the Laminare hood, which is equipped with a 20× Nikon lens. The fibers are viewed using the microscope eyepiece and/or an attached Sony Trinitron video monitor. The inter-fiber spacing is checked using the Quadra-Chek 200 device attached to the microscope. Using the thumb wheel, the fiber pin blocks are rotated by small increments, allowing approximately 5 min between increments. Since the tape adhesive is viscoelastic, rotating the fiber pin blocks too fast results in breaking of some of the fibers. Once the desired inter-fiber spacing is achieved, the thumb wheel is locked in place using the stop screw. The height of the fiber placement stage is then raised, using the “Z” motion set screws, to a level that puts the fiber mold close to the plane of the rotated fibers. A central cavity is then selected, and the mold is adjusted so that the fiber array is centrally located within the sprue slots of this cavity. After this procedure, the mold is then secured to the stage with tape (see Fig. 4).

To prepare combinatorial microcomposites, this rotated fiber array is now discarded along with the tape placed on the outside edge of the fiber pin block. With the mold

securely in place on the stage of the fiber placement device, the device is removed from the microscope stage and placed on the workspace of the hood. Single fibers are then placed at the outer edges of each sprue slot in the mold and secured to the double-sided stick tape that was placed on the beams that parallels the fiber mold. After this procedure, additional tape can be placed over these single fibers to minimize movement. For the molds used in this laboratory, the width of the sprue slots varies from 0.381 to 1.778 mm (0.015–0.070 in). Therefore, the distance between these two parallel single fibers varies from 350 to 1,750 μm . The orientation of the mold prior to placement of the single fibers is made in such a way as to ensure that the single fibers will be parallel to the multifiber array.

The mold is then lowered and another multifiber array is prepared as described previously. After raising the mold to the approximate plane of the rotated fibers, the multifiber array is centered in the sprue slots of the desired cavity between the two parallel single fibers. While following the effect of each height increase with the measurescope, the “Z” motion set screws are then adjusted slowly to keep the base of the sprue slots, and hence the mold, at a level relative to the plane of the fibers. This minimizes movement of the fibers when they make contact with the surface of the sprue slot. The location of the fiber array is then secured in the mold by attaching them to the double-sided stick tape on the beam that parallels the fiber mold.

To prepare 3-D microcomposites, the first-row fibers are placed on alternate pins of the fiber pin blocks (i.e., the # 1, 3, 5, and 7 pins) and temporarily secured on the double stick tape (see Fig. 5). Once the first row is completed, double stick tape is placed on top of the first row of fibers attached to the fiber pin blocks to secure the fibers but still allowing the fibers to slip between the two pieces of tape

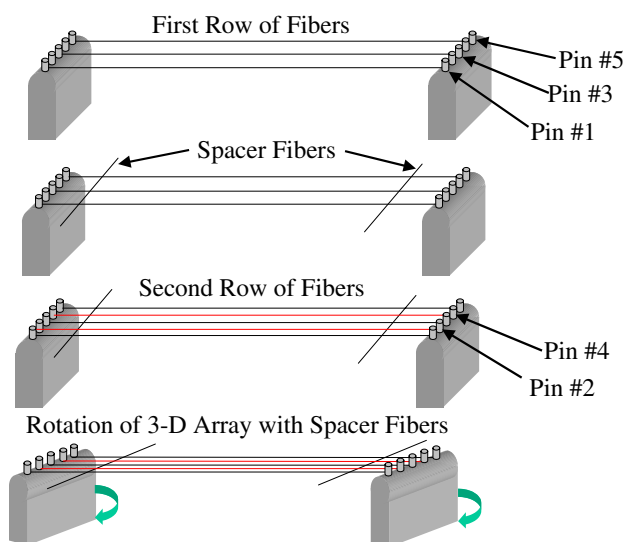


Fig. 5 Graphical depiction of 3-D fiber rotation procedure

during the rotation process. Two glass or carbon fibers are then placed across the first row of fibers to act as spacers. The spacer fibers are located approximately above the first channel outside the mold cavity. A second row of fibers is then placed across the empty pins (i.e., # 2, 4, 6, and 8 pins) on top of the fiber spacers. These fibers are also secured on the second layer of double-sided stick tape that has been placed on the fiber pin block. This process can now be repeated to make as many rows as desired. After the final row is completed, the double-sided sticky tape is placed on top of this row to secure these fibers. During the sequential rotation of the fiber array, the spacer fibers, by holding the fiber ends, are adjusted to keep them above the first channel.

The 3-D array is rotated until the inter-fiber distance between fibers on each row is approximately 50 μm . As before, the height of the fiber placement stage is then raised, using the “Z” motion set screws, to a level that puts the fiber mold close to the plane of the rotated fibers. A mold cavity is then selected and the mold is adjusted so that the fiber array is centrally located within the sprue slots of this cavity. At this time, the spacer fibers are adjusted to ensure that they are aligned with the first channel outside of the cavity. The array is then placed in the mold cavity by slowly adjusting the “Z” motion set screws to keep the base of the sprue slots, and hence the mold, at a level relative to the plane of the fibers.

For 2-D microcomposites, the coefficient of friction between the fibers and base of the sprue slot is sufficient to minimize movement of the fibers in the array when the fibers are secured in the mold cavity using 5-min epoxy. For 3-D microcomposites, 5-min curing epoxy diluted with acetone is placed on top of the array above the spacer fibers after the first row of fibers in the array touches the base of the sprue slot. In addition to facilitating the penetration of the resin between the fibers in the array, the reduced viscosity of the 5-min epoxy allows the tensioned fibers to readjust to the appropriate array spacing after application of the epoxy. After the epoxy is dry, undiluted 5-min epoxy is then placed between the first and second channels to firmly secure the fibers in the mold cavity.

Combinatorial multifiber arrays

An example of a 2-D combinatorial microcomposite containing a four-fiber array and two single fibers is shown in Fig. 6. In this figure, the expanded region of the 2-D, four-fiber array shows that the inter-fiber distance is uniform. Using an average fiber diameter of 15 μm , the inter-fiber distance within the array is approximately 1.4 fiber diameters, ϕ . The two single fibers are 710 and 905 μm i.e., 47ϕ and 60ϕ , respectively, from the multifiber array.

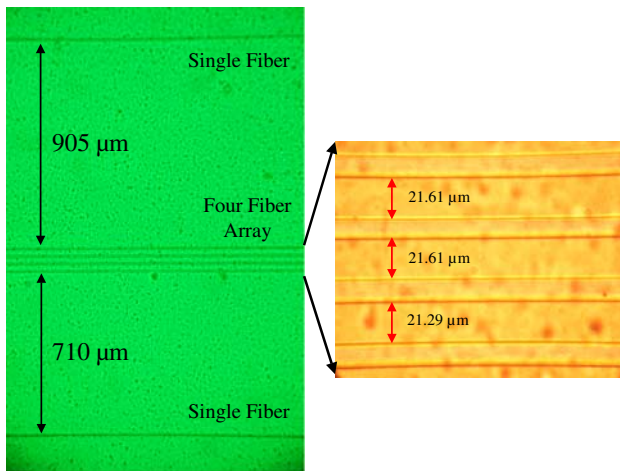


Fig. 6 Typical 2-D combinatorial microcomposite

Based on previous research [9], no interaction between the single fibers and the multifiber array should be observed. Therefore, the impact of fiber–fiber interactions upon fiber fracture can be evaluated relative to the single fiber fragmentation under identical deformation regimes. From these types of specimens and with the appropriate testing device, one may simultaneously evaluate the interfacial shear strength (IFSS) and its apparent change due to inter-fiber interactions. In addition, the impact of IFSS and interphase toughness on critical flaw nucleation can also be evaluated in the 2-D and 3-D microcomposite arrays relative to the response one obtains from the SFF test.

Figure 7 shows a typical two-layer 3-D microcomposite and the view of the inter-fiber spacing and layering from an

edge on specimen taken from the tab section of the dog-bone specimens. The top and bottom rows of the two-layer 3-D microcomposite are shown in focus in Fig. 7a, b, respectively. To aid the eye in discerning the in-focus fibers, small symbols are placed to the left and right, respectively, of each image. Note that the inter-fiber distance between each layer is not as uniform as observed in the 2-D array. This is primarily due to the gluing procedure with some contribution due to imperfection of the pin spacing in the fiber pin block. However, the edge view of the array (see Fig. 7c) shows that the layers are distinct and separated by approximately 1.6ϕ . Arrows are used to aid the reader in seeing these fibers since the indexes of refraction of the glass fiber and epoxy resin are similar. With the inter-fiber spacing achieved for the 3-D microcomposite, it is likely that effective fiber volume fractions exceeding 0.5 can be achieved by 3-D multifiber arrays.

It is generally accepted that a weak fiber/matrix interface increases composite toughness, while a strong interface increases composite strength but leads to reduced toughness. This is presumably due to the tendency of strong interfaces to form matrix cracks during fiber fracture, which accelerates the nucleation of critical cracks. Holmes and McDonough [29] have demonstrated an example of time-dependent critical flaw nucleation in a 2-D multifiber array where fiber fracture is accompanied by matrix crack formation. In Fig. 8, a 2-D multifiber array is subject to a strain of approximately 3%, well below the 6% failure strain of the resin. The failure was shown to occur by the coalescence of two matrix cracks occurring on the same fiber break plane.

Fig. 7 Optical microscopic image shows top (a) and bottom row (b) in typical two-layer 3-D microcomposite. Edge on view taken from tab region of the dogbone specimen (c)

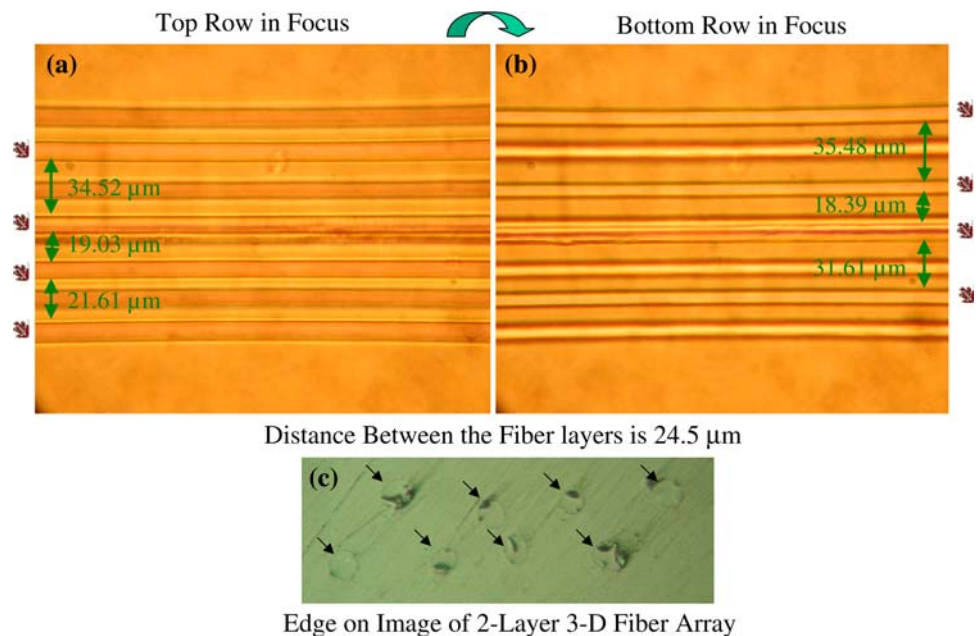


Fig. 8 Collage showing the evolution of fiber breaks with time in a 2-D multifiber array at a constant strain of approximately 3%. The specimen was taken to approximately 3% strain by sequential strain steps. In Fig. 8a, the fibers are numbered according to the convention adopted by Sastry and Phoenix [30] (reproduced with permission from reference [27])



Interestingly, matrix toughness has been identified as a key parameter for increasing damage tolerance in advanced composites [31]. However, the factors that control this increase in toughness are not well understood. Micromechanics research on 2-D and 3-D microcomposites may prove invaluable in quantifying how the matrix influences

damage tolerance; however, larger 3-D arrays must be prepared and instruments capable of archiving the data from the many fiber fracture events that occur prior to critical flaw nucleation must be developed. At present, a nontedious methodology for preparing these large 3-D arrays remains to be developed.

References

1. Zhao FM, Okabe T, Takeda N (2000) *Compos Sci Technol* 60:1965
2. Zhao FM, Takeda N (2000) *Compos A Appl Sci Manuf* 31:1215
3. Rosen WB, Dow NF, Hashin Z (1964) Mechanical properties of fibrous composites; NASA CR-31. General Electric Company, Philadelphia, PA
4. Rosen WB (1964) *Am Inst Aeronaut Astronaut* 2:1985
5. W. B. Rosen (1965) In: American Society of Metals (ed) *Fiber composite materials*, chap 3. American Society of Metals, Metals Park, Ohio, p 37
6. Zweben C (1968) *Am Inst Aeronaut Astronaut J* 6:2325
7. Zweben C, Rosen BW (1970) *J Mech Phys Solids* 18:189
8. Mullin J, Berry JM, Gatti A (1968) *J Compos Mater* 2:82
9. Li ZF, Grubb DT, Phoenix SL (1995) *Compos Sci Technol* 54:251
10. Wagner HD, Steenbakkens LW (1989) *J Mater Sci* 24:3956. doi: [10.1007/BF01168959](https://doi.org/10.1007/BF01168959)
11. Jones KD, Dibenedetto AT (1994) *Compos Sci Technol* 51:53
12. Grubb DT, Li ZF, Phoenix SL (1995) *Compos Sci Technol* 54:237
13. van den Heuvel PWJ, Peijs T, Young RJ (1996) *J Mater Sci Lett* 15:1908
14. van den Heuvel PWJ, van der Bruggen YJW, Peijs T (1996) *Compos A Appl Sci Manuf* 27:855
15. van den Heuvel PWJ, Peijs T, Young RJ (1997) *Compos Sci Technol* 57:899
16. van den Heuvel PWJ, Wubbolts MK, Young RJ, Peijs T (1998) *Compos A Appl Sci Manuf* 29:1121
17. van den Heuvel PWJ, Peijs T, Young RJ (1998) *Compos Sci Technol* 58:933
18. van den Heuvel PWJ, Peijs T, Young RJ (2000) *Compos A Appl Sci Manuf* 31:165
19. Schadler LS, Galiotis C (1995) *Int Mater Rev* 40:116
20. Schadler LS, Amer MS, Iskandarani B (1996) *Mech Mater* 23:205
21. Ibnabdeljalil M, Curtin WA (1997) *Int J Solids Struct* 34:2649
22. Landis CM, Beyerlein IJ, McMeeking RM (2000) *J Mech Phys Solids* 48:621
23. Curtin WA, Takeda N (1998) *J Compos Mater* 32:2060
24. Mahesh S, Phoenix SL, Beyerlein IJ (2002) *Int J Fract* 115:41
25. Smith RL, Phoenix SL, Greenfield MR, Henstenburg RB, Pitt RE (1983) *Proc R Soc Lond A Math Phys Eng Sci* 388:353
26. Otani H, Phoenix SL, Petrina P (1991) *J Mater Sci* 26:1955. doi: [10.1007/BF00543630](https://doi.org/10.1007/BF00543630)
27. Holmes GA, Feresenbet E, Raghavan D (2003) *Compos Int* 10:515
28. Drzal LT, Herrera-Franco PJ (1990) In *Engineered materials handbook: adhesives and sealants*, ASM Int.: Metals Park, Ohio, p 391
29. Holmes GA, McDonough WG (2002) In: Rasmussen BM, Pilato LA, Kliger HS (eds) *Proceedings of the 47th international SAMPE symposium and exhibition—Science of the advance materials and process engineering series*, Society for the Advancement of Material and Process Engineers (SAMPE), Covina, CA, May 2002, p 1690
30. Sastry AM, Phoenix SL (1993) *J Mater Sci Lett* 12:1596
31. Sierakowski RL, Newaz GM (1995) *Damage tolerance in advanced composites*. Technomic Publishing Co., Inc, Lancaster, PA